# Plasmodium berghei NK65 induces cerebral leukocyte recruitment in vivo: An intravital microscopic study

Norinne Lacerda-Queiroz [a,b], Onésia Cristina Oliveira Lima [b], Cláudia Martins Carneiro [d], Márcia Carvalho Vilela [c], Antônio Lúcio Teixeira [e], Andrea Teixeira-Carvalho [f], Márcio Sobreira Silva Araújo [f], Olindo Assis Martins-Filho [f], Érika Martins Braga [a], Juliana Carvalho-Tavares [b,*]

[a] Departamento de Parasitologia, Universidade Federal de Minas Gerais, Minas Gerais, Brazil
[b] Núcleo de Neurociências, Departamento de Fisiologia e Biofísica, Universidade Federal de Minas Gerais, Minas Gerais, Brazil
[c] Laboratório de Imunofarmacologia, Departamento de Bioquímica e Imunologia, Instituto de Ciências Biológicas, Universidade Federal de Minas Gerais, Minas Gerais, Brazil
[d] Laboratório de Imunopatologia, Núcleo de Pesquisas em Ciências Biológicas, Departamento de Análises Clínicas, Escola de Farmácia, Universidade Federal de Ouro Preto, Minas Gerais, Brazil
[e] Departamento de Clínica Médica da Faculdade de Medicina, Universidade Federal de Minas Gerais, Minas Gerais, Brazil
[f] Laboratório de Biomarcadores de Diagnóstico e Monitoração, Centro de Pesquisas René Rachou, Fundação Oswaldo Cruz, Minas Gerais, Brazil

## ARTICLE INFO

## ABSTRACT

Malaria is second only to tuberculosis as the leading cause of morbidity and mortality as a consequence of a single infectious agent. Much of the pathology of malaria arises from the inappropriate or excessive immune response mounted by the host in an attempt to eliminate the parasite. We here report the inflammatory changes observed in the cerebral microvasculature of C57BL/6 and BALB/c mice that had been inoculated with Plasmodium berghei NK65, a lethal strain of rodent malaria. Although no neurological signs were observed in experimentally infected mice, inflammation of the cerebral microvasculature was clearly evident. Histopathological analysis demonstrated that alterations in cerebral tissue were more intense in infected C57Bl/6 mice than in infected BALB/c animals. Intravital microscopic examination of the cerebral microvasculature revealed increased leukocyte rolling and adhesion in pial venules of infected mice compared with non-infected animals. The extravasation of Evans blue dye into the cerebral parenchyma was also elevated in infected mice in comparison with their non-infected counterparts. Additionally, protein levels of TNF-α, MIG/CXCL9, MCP-1/CCL2, MIP-1α/CCL3 and RANTES/CCL5 were up-regulated in brain samples derived from infected C57Bl/6 mice. Taken together, the data reported here illustrate the complex strain-dependent relationships between leukocyte recruitment, blood brain barrier permeability and chemokine production.

© 2011 Elsevier B.V. All rights reserved.

## 1. Introduction

Malaria is one of the most important tropical parasitic diseases and remains a major human health problem. It is estimated that some 500 million episodes of clinical Plasmodium falciparum malaria occur annually on a worldwide basis (Snow et al., 2005), but the greatest impact is in sub-Saharan Africa where millions of children die every year (World Health Organisation, 2000). Complications that commonly follow infection by P. falciparum may give rise to severe malaria, the pathology of which is multi-factorial and complex, and typically includes one or more of the following manifestations: cerebral malaria (CM), severe anaemia, acute renal failure, respiratory distress syndrome, circulatory collapse, haemoglobinuria and metabolic acidosis (Miller et al., 2002; Hunt et al., 2006).

Most studies of CM have involved murine models in which animals are experimentally infected with a Plasmodium strain (de Souza and Riley, 2002). In this context, the parasite strain Plasmodium berghei ANKA (PbA) produces a clear division between resistant (BALB/c and A/J) and susceptible (C57Bl/6 and CBA) strains of mice (Grau et al., 1990). Although such animal models do not reproduce the human disease exactly, they do exhibit some histopathological similarities including changes in the cerebral microvasculature, breakdown of the blood–brain barrier (BBB), petechial haemorrhages, congestion and oedema.

* Corresponding author at: Departamento de Fisiologia e Biofísica, ICB, UFMG, 31270-901 Av. Antônio Carlos, 6627, Pampulha, Belo Horizonte, MG, Brazil. Tel.: +55 31 3409 2943; fax: +55 31 3409 2924.

E-mail addresses: norinneq@yahoo.com.br (N. Lacerda-Queiroz), onesiacristina@yahoo.com.br (O.C.O. Lima), carneirocm@gmail.com (C.M. Carneiro), marciacvilela@gmail.com (M.C. Vilela), altexr@gmail.com (A.L. Teixeira), andreat@cpqrr.fiocruz.br (A.T. Carvalho), sobreira@cpqrr.fiocruz.br (M.S.S. Araújo), oamfilho@cpqrr.fiocruz.br (O.A. Martins-Filho), embraga@icb.ufmg.br (É.M. Braga), julianat@icb.ufmg.br (J. Carvalho-Tavares).

The central nervous system (CNS) is considered to be an immunologically privileged site since it is protected, under normal physiological conditions, from leukocyte transfer by the BBB. However, during inflammatory conditions the integrity of the BBB may be compromised allowing mononuclear cells and proteins, including cytokines, to gain access to the CNS more freely (Saunders et al., 2008). It has previously been shown that the inflammatory response in experimental cerebral malaria (ECM) is not due to the infection itself but is rather a consequence of a strong immune reaction by the host involving the release of cytokines (Grau et al., 1987, 1989).

Although the evidence for a crucial role of TNF in the pathogenesis of CM is strong, the occurrence of high plasma levels of the cytokine in human and mouse malaria infections without cerebral complications (Shaffer et al., 1991; Karunaweera et al., 1992; Clark et al., 1990) and the failure of the TNF antibody trial in Gambian children (Van Hensbroek et al., 1996) have been perplexing. Indeed, recently, it was shown that $LT\alpha^{-/-}$ mice are protected against CM induced by *P. berghei* ANKA, whereas $TNF^{-/-}$ mice are not (Engwerda et al., 2002).

However, the chemokines, a group of chemoattractant cytokines, are also known to mediate protozoan parasite infections through interactions between the parasite and host cells and by influencing the immune system (Brenier-Pinchart et al., 2001). Indeed, leukocyte recruitment to sites of inflammation involves the participation of chemokines, which regulate the expression of adhesion molecules and their ligands involved in leukocyte migration along a concentration gradient (Ono et al., 2003; Pease and Williams, 2006).

Intravital microscopy has been used in a range of animal models to investigate, *in vivo* in the systemic circulation, the interactions between circulating leukocytes and endothelial cells in a wide range of inflammatory models (Scheiermann et al., 2009; dos Santos et al., 2008). The aim of the present study was, therefore, to evaluate the inflammatory responses induced in the cerebral microcirculatory by infection with a malaria strain that is known not to induce ECM – *P. berghei* NK65 (Yoshimoto et al., 1998) – because we intended to assess the level, if any, of cerebral microvascular inflammation in the absence of the more severe changes typical of ECM. We also chose to use two mouse strains, BALB/c and C57Bl/6, to expose any strain-related differences in cerebral microvascular inflammation, in the absence of ECM. The microvascular inflammation was characterised in terms of histological changes, cerebral leukocyte recruitment, phenotyping of infiltrated cerebral leukocytes, release of cytokines and chemokines, and the integrity of the BBB.

## 2. Materials and methods

Details of the project, including procedures for animal care and experimental protocols, were submitted to and approved by the Animal Ethics Committee of the Instituto de Ciências Biológicas, Universidade Federal de Minas Gerais (UFMG), Brazil (application number 005/05).

### 2.1. Animals and parasites

Six week-old female mice (strains BALB/c and C57Bl/6) were obtained from the Animal Care Facilities of UFMG, and housed under standard conditions with free access to commercial chow and water.

Malaria parasites were stored as frozen stocks in liquid nitrogen. *P. berghei* NK65 is an uncloned line of high-virulence strain and was originally obtained from Dr. Luzia H. Carvalho (Centro de Pesquisas René Rachou, Fiocruz MG, Belo Horizonte, MG, Brazil). Parasitized RBCs (pRBCs) of *P. berghei* NK65 were generated in donor BALB/c background mice inoculated intraperitoneal (i.p.) with frozen stock of parasites as reported previously (Laranjeiras et al., 2008). The donor mice were monitored for parasitemia daily and bled for experimental infection in ascending periods of parasitemia.

### 2.2. Infection of experimental animals

Mice (BALB/c or C57Bl/6) were infected by intraperitoneal (i.p.) injection of $10^6$ parasitised red blood cells, from donor mice, suspended in 0.2 mL phosphate buffered saline (PBS) (Grau et al., 1986). Parasitemia levels in infected mice were monitored on Giemsa-stained blood smears from the 3rd day post infection (dpi) onwards and estimated over 1000 red blood cells. The body weights of experimental animals were monitored from the start of the experiment until death.

### 2.3. Brain histopathology

At 3, 6 and 9 dpi, infected and non-infected mice of both strains were euthanised, following which brains were removed rapidly, fixed in 10% formalin, embedded in paraffin and cut into 4 μm sagittal sections. Slides were stained with hematoxylin and eosin, and cerebral oedema, congestion, death of endothelial cells, parenchymal haemorrhage, proliferation of glia, accumulation of erythrocytes and leukocyte adhesion were evaluated in the cortex area under a light microscope.

### 2.4. Intravital microscopy

Intravital microscopy of the cerebral microvasculature was performed on 5 dpi as described previously (Carvalho-Tavares et al., 2000). Briefly, infected ($n=6$) and non-infected ($n=6$) of both strains were anaesthetised by ip injection of a mixture of ketamine (150 mg/kg; Laboratório Cristália, Itapira, SP, Brazil) and xylazine (10 mg/kg; Rompun®; Bayer, São Paulo, SP, Brazil) and the tail veins were cannulated for the intravenous administration of rhodamine 6G (0.3 mg/kg; Sigma, St. Louis, MO, USA) (Baatz et al., 1995). Craniotomies were performed using a high-speed drill (Dremel, Racine, WI, USA) and dura matter removed to expose the underlying pial vasculatures. During this procedure, the experimental animals were maintained at 37 °C with the aid of heating pads (Fine Science Tools Inc., North Vancouver, BC, Canada), and the exposed brain tissue was continuously superfused (0.5 mL/min; 37 °C) with artificial cerebrospinal fluid buffer (132 mM NaCl, 2.95 mM KCl, 1.71 mM $CaCl_2$, 0.64 mM $MgCl_2$, 24.6 mM $NaHCO_3$, 3.71 mM dextrose, and 6.7 mM urea; pH 7.4).

In order to observe leukocyte–endothelium interactions, leukocytes that had been fluorescently labelled with rhodamine 6G were visualised using an Olympus (Center Valley, PA, USA) model BX40 microscope fitted with a fluorescent light source (epi-illumination at 510–560 nm using a 590 nm emission filter) and a silicon-intensified camera (Optronics Engineering, Goleta, CA, USA), the output from which was displayed on an Olympus monitor. Rolling leukocytes (cells/min) were defined as white cells moving at a velocity less than that of erythrocytes. Leukocytes were considered to be adherent to the venular endothelium (100 μm) if they remained stationary for 30 s or longer.

### 2.5. Isolation of brain cells and immunophenotyping

Animals were anesthesized and perfused with PBS in order to wash out cells in the lumen of the blood vessels; thus the cells in this preparation represent cells located in the brain parenchyma. Each sample ($n$) correspond a pool of two mice brains. The fragments of the brain were immersed in cold RPMI-1640 in Petri dish and placed
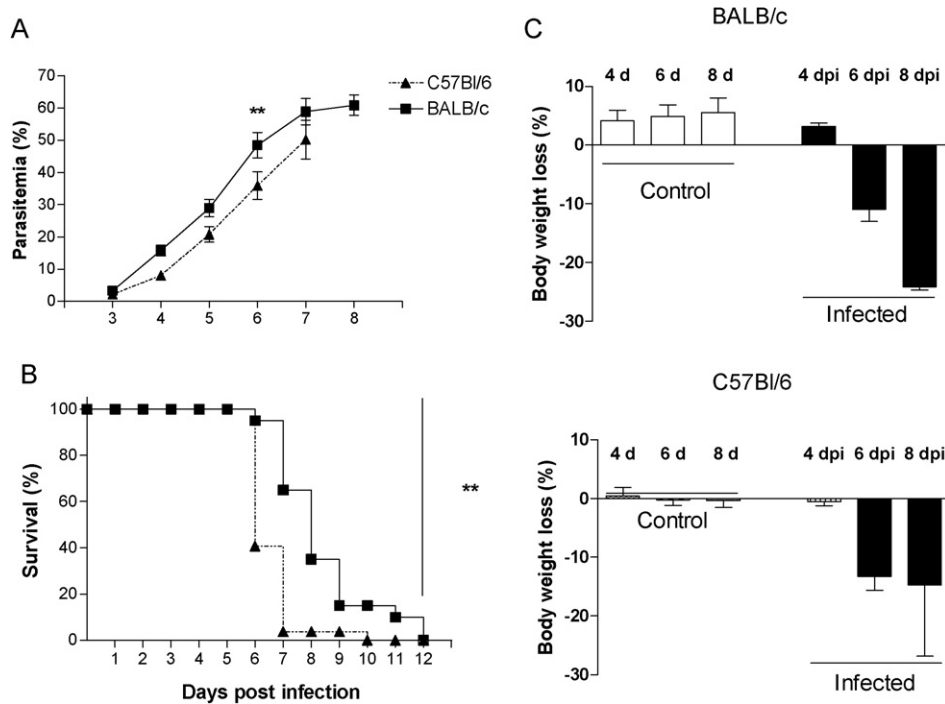
**Fig. 1.** Course of *P. berghei* NK65 infection in BALB/c and C57Bl/6 mice, showing: (A) parasitemia levels (mean ± SEM) measured on Giemsa-stained blood smears from 3 dpi onwards, with $p < 0.05$ on 6 dpi; (B) survival rate during infection, with a different profile ($p < 0.05$) between C57Bl/6 and BALB/c mice; and (C) variation in body weight expressed as a percentage of the initial weight [for control mice, timing (d) relates to dpi for experimental animals]. Parasitemia was evaluated by Two-way ANOVA with Bonferroni post-test and the Kaplan Meier was used to estimate survival.

on ice. The tissues were pressed using surgical tweezers and then filtered on stainless steel gauze to obtain single cell suspensions, according to the protocol of Teixeira-Carvalho (Teixeira-Carvalho et al., 2002) with some modifications. The cell suspension was centrifuged at $200 \times g$ for 10 min at 4 °C and the supernatant containing cell debris was removed. The leukocyte pellet was washed once in RPMI-1640 and centrifuged at $400 \times g$ for 10 min at 4 °C. The cell pellet was resuspended in 700 μL RPMI-1640. The cells were stained in a dual-colour immunocytometric assay using fluorescein isothiocyanate (FITC) and peridin-chlorophyll protein (PerCP)-conjugated mAbs. In this study, we used anti-mouse CD4-FITC, CD8-FITC, CD69-PE CD19-FITC, NK1.1-FITC, CD3-PerCP. Monoclonal antibodies were purchased from Becton-Dickinson (Mountain View, CA, USA) or DAKO (Carpinteria, CA, USA). The cells were incubated with 2 μL mAbs on ice for 30 min. After staining, the erythrocytes in the sample were lysed with FACS Lysing Solution (Becton-Dickinson). The cell suspensions were then fixed using FACS Fix Solution (10 g/L of paraformaldehyde, 10.2 g/L of sodium cacodilate and 6.63 g/L of sodium chloride, pH 7.2, all from Sigma, St Louis, MO, USA). The cell phenotypes were analyzed by flow cytometry, using FACScan (Becton–Dickinson) and CELLQUEST software for data acquisition and analysis. The results were express as % cells/g of brain, because it is tissue extracts not serum/plasma.

The values represent the means and standard errors of the means ($n = 4$ mice/each group).

### 2.6. Evaluation of BBB integrity

The integrity of the BBB was investigated using Evans-Blue (EB) dye as a marker of albumin extravasation into tissue as reported previously (Belayev et al., 1996). At 5 dpi, infected and non-infected mice of both strains were injected intravenously with 0.2 mL of 2% EB in saline, euthanised 1 h later and perfused with 5 mL of saline. Brain samples were removed, weighed, dried at 37 °C for 48 h and EB extracted by incubation in 1 mL of formamide at 25 °C for 48 h.

The amounts of EB in the extracts were measured colorimetrically at 620 nm with the aid of an ELISA plate reader. Results are presented as the amount of Evans blue (pg) present in 100 mg (dry weight) of brain tissue.

### 2.7. Determination of cytokines and chemokines in brain and serum samples

At 5 dpi, infected and non-infected mice of both strains were euthanised, following which brains were removed and homogenised (Ultra-Turrax) in extraction solution (0.4 M NaCl, 0.05% Tween 20, 0.5% BSA, 0.1 mM phenylmethylsulphonyl fluoride, 0.1 mM benzethonium chloride, 10 mM EDTA and 20 KI units aprotinin) at the rate of 1 mL per 100 mg of brain tissue. The resulting homogenates were centrifuged at $3000 \times g$ for 10 min at 4 °C and the supernatants collected and stored at −70 °C. The concentrations of TNF-α, IFN-γ, Kc/CXCL1, MIG/CXCL9, MIP-1α/CCL3, MCP-1/CCL2 and RANTES/CCL5 were assayed by ELISA using commercially available antibodies (R&D Systems, Minneapolis, MN, USA; Pharmingen, San Diego, CA, USA) employed according to the procedures supplied by the manufacturers. The samples were tested in duplicate.

The systemic, circulating levels of TNF-α were also measured in serum samples derived from the coagulated blood (15 min at 37 °C, then 30 min at 4 °C) of some experimental animals. Serum was stored at −20 °C until required for use and diluted (1:3) in 1% BSA in PBS prior to assay.

### 2.8. Statistical analysis

Data are shown as mean ± SEM (except the survival curve). Leukocyte-endothelium interaction, evaluation of BBB breakdown and ELISA results were evaluated by ANOVA, with Bonferroni post-test. Parasitemia was evaluated by Two-way ANOVA with Bonferroni post-test and the Kaplan Meier estimator was used to estimate survival. Differences were considered to be significant for $p$ values <0.05.
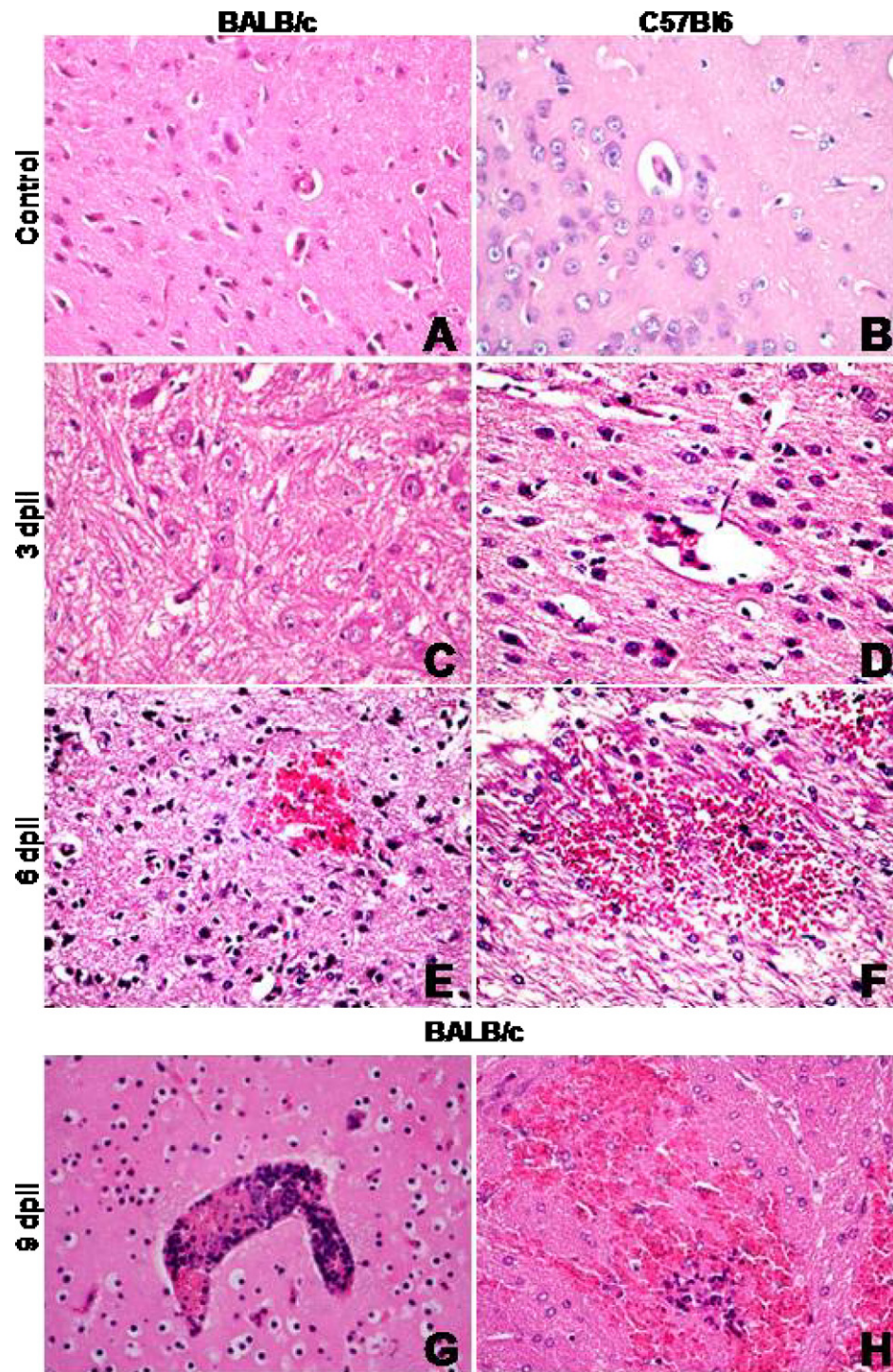
**Fig. 2.** Histopathological evaluation of the brain during the course of *P. berghei* NK65-infection in mice. Panels (A) and (B) show brain sections of non-infected control BALB/c and C57Bl6 mice, respectively. Brain sections from infected BALB/c mice on 3 dpi (panel C) demonstrate that there were no alterations *cf.* with the control (panel A), whilst in samples from infected C57Bl/6 mice (panel D) the vessels had leukocytes adhered to the endothelium. On 6 dpi, there were diffuse inflammatory cells and mild hemorrhagic foci in infected BALB/c mice (panel E), but intense hemorrhagic foci in infected C57Bl/6 mice (panel F). By 9 dpi, there were erythrocytes and leukocytes adhered to the endothelium (panel G) and intense hemorrhagic foci (panel H) in infected BALB/c animals. All slides were stained with hematoxylin and eosin and are shown at a magnification of 600×.

## 3. Results

### 3.1. Course of P. berghei NK65 infection in BALB/c and C57Bl/6 mice

Parasitemia levels in BALB/c and C57Bl/6 mice that had been infected with *P. berghei NK65* showed progressive increases from 3 dpi until death (Fig. 1A). Although parasitemia was significantly higher in BALB/c than in C57Bl/6 ($p < 0.05$) animals on 6 dpi, the survival rate showed a different profile ($p < 0.05$) with earlier deaths of C57Bl/6 mice compared with their BALB/c counterparts (Fig. 1B). Significant weight losses were detected in all infected mice in comparison with the respective non-infected (control) groups (Fig. 1C).

## 3.2. Brain histopathology

The progress of morphological changes in brain samples of *P. berghei* NK65 infected BALB/c and C57Bl/6 animals were evaluated using histopathological techniques on 3, 6 and 9 dpi. Signs of cerebral oedema, congestion, death of endothelial cells, parenchymal haemorrhage, proliferation of glia, accumulation of erythrocytes and leukocyte adhesion were detected in some samples. In comparison with non-infected animals (Fig. 2B), infected C57Bl/6 mice showed mild tissue alterations as early as 3 dpi (Fig. 2D), whilst samples from infected BALB/c mice (Fig. 2C) were indistinguishable from those of the respective control group (Fig. 2A) at this time. On 6 dpi, however, infected BALB/c animals presented moderate changes (Fig. 2E), whilst infected C57Bl/6 mice showed more severe and progressive alterations (Fig. 2F). Tissue modifications in brain samples from the infected BALB/c animals that had survived to 9 dpi (Figs. 2G and H) were similar to, and as intense as, those observed in infected C57Bl/6 mice on 6 dpi.

## 3.3. Leukocyte recruitment in the pial microvasculature

Since histopathological assessment had revealed that initial inflammatory events were present in both strains after 4 dpi, leukocyte–endothelium interactions were assessed on 5 dpi. Intravital microscopy of the pial microvasculature revealed significant increases ($p < 0.05$) in leukocyte rolling (Fig. 3A) and adhesion (Fig. 3B) in both infected strains compared with non-infected controls, except for C57Bl/6 adhesion. However, leukocyte rolling was significantly enhanced ($p < 0.01$) and leukocyte adhesion significantly reduced ($p < 0.05$) in infected C57Bl/6 mice in comparison with infected BALB/c animals.

## 3.4. Immunophenotyping of leukocytes in brain cell suspension

In order to establish what type of lymphocytes had rolled or adhered in the microvessels in C57BL/6 or BALB/c mice had then migrate into the brain parenchyma, the percentage of lymphocyte subsets within the total brain cell suspension in these mice was investigated by flow cytometry (Fig. 4B). These cell suspensions were prepared after perfusing the brains with PBS (see Section 2). The results demonstrated that C57Bl/6 *P. berghei* NK65 infection (on 5 dpi) is accompanied by a significant increased percentage of B CD19$^+$ lymphocytes as compared to the non-infected control animals (Fig. 4A). In contrast, the BALB/c *P. berghei* NK65 infection (on 5 dpi) is accompanied by a decreased percentage of both T CD3$^+$ and T CD4$^+$ lymphocytes (Fig. 4B) as well as B CD19+ lymphocytes as compared to the non-infected control animals. No significant difference was observed in the percentage of CD3$^+$, CD4$^+$, CD3$^+$CD69$^+$ or CD3-NK1.1$^+$ cells between the two evaluated groups in both C57Bl6 and BALB/c mice.

Data from the frequency of leucocytes on the brain cell suspension also demonstrated that T CD3$^+$ lymphocytes is the most predominant cell type present on the brain leukocyte subpopulations in infected animals (Fig. 4A).

## 3.5. Evaluation of vascular permeability

At 5 dpi, significant increases ($p < 0.01$) in EB dye extravasation (Fig. 5) into the cerebral parenchyma of infected animals of both strains were observed in relation to the respective non-infected controls, but no strain-related differences in BBB permeability were detected at this time.

### 3.5.1. Cytokine and chemokine concentrations

Levels of TNF-α, IFN-γ, MCP-1/CCL2, Kc/CXCL1, MIG/CXCL9, RANTES/CCL5 and MIP-1α/CCL3 were determined in brain extracts
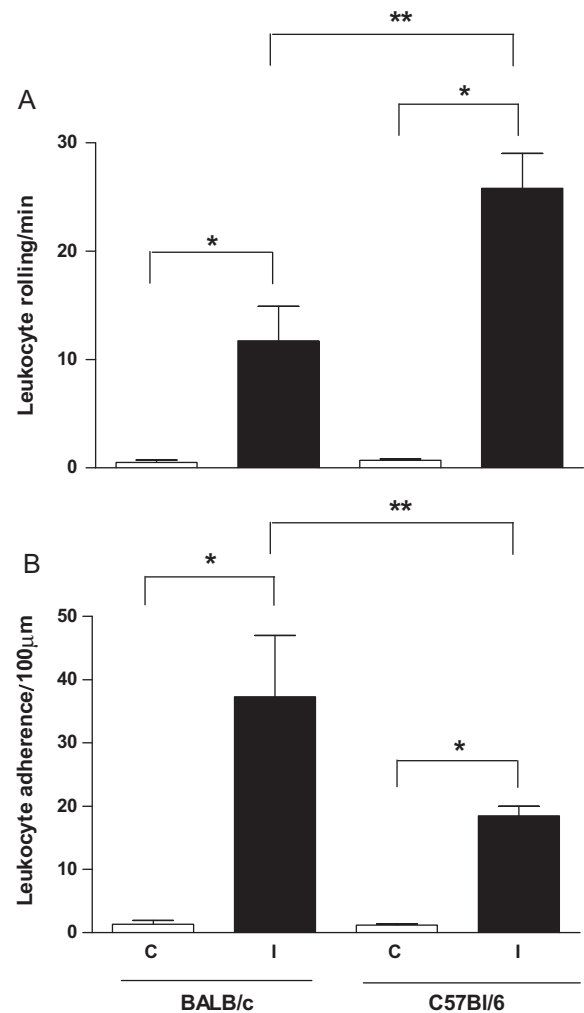


**Fig. 3.** Evaluation of leukocyte-endothelium interactions by intravital microscopy, showing: (A) leukocyte rolling and (B) leukocyte adhesion in the brain microvasculature of BALB/c and C57Bl/6 mice on 5 days after infection with *P. berghei* NK65 (bars labelled I) and in respective non-infected control mice (bars labelled C). Mean and ±SEM values for groups of at least six mice. The results were evaluated by ANOVA, with Bonferroni post-test. Significant differences ($p < 0.05$) between infected and control mice are marked (*), whilst differences between infected groups are marked (**).
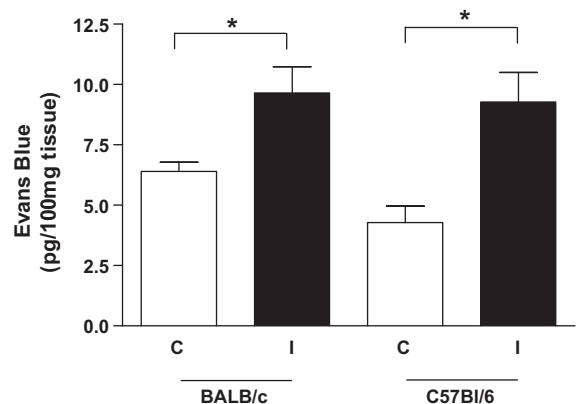


**Fig. 5.** Evaluation of BBB breakdown by determination of the concentration of Evans blue in cerebral parenchyma, showing vascular permeability in the brains of BALB/c and C57Bl/6 mice on day 5 after infection with *P. berghei* NK65 (bars labelled I) and in respective non-infected control mice (bars labelled C). Mean and ±SEM values for groups of at least six mice are shown. The results were evaluated by ANOVA, with Bonferroni post-test. Significant differences ($p < 0.05$) between infected and control mice are marked (*).
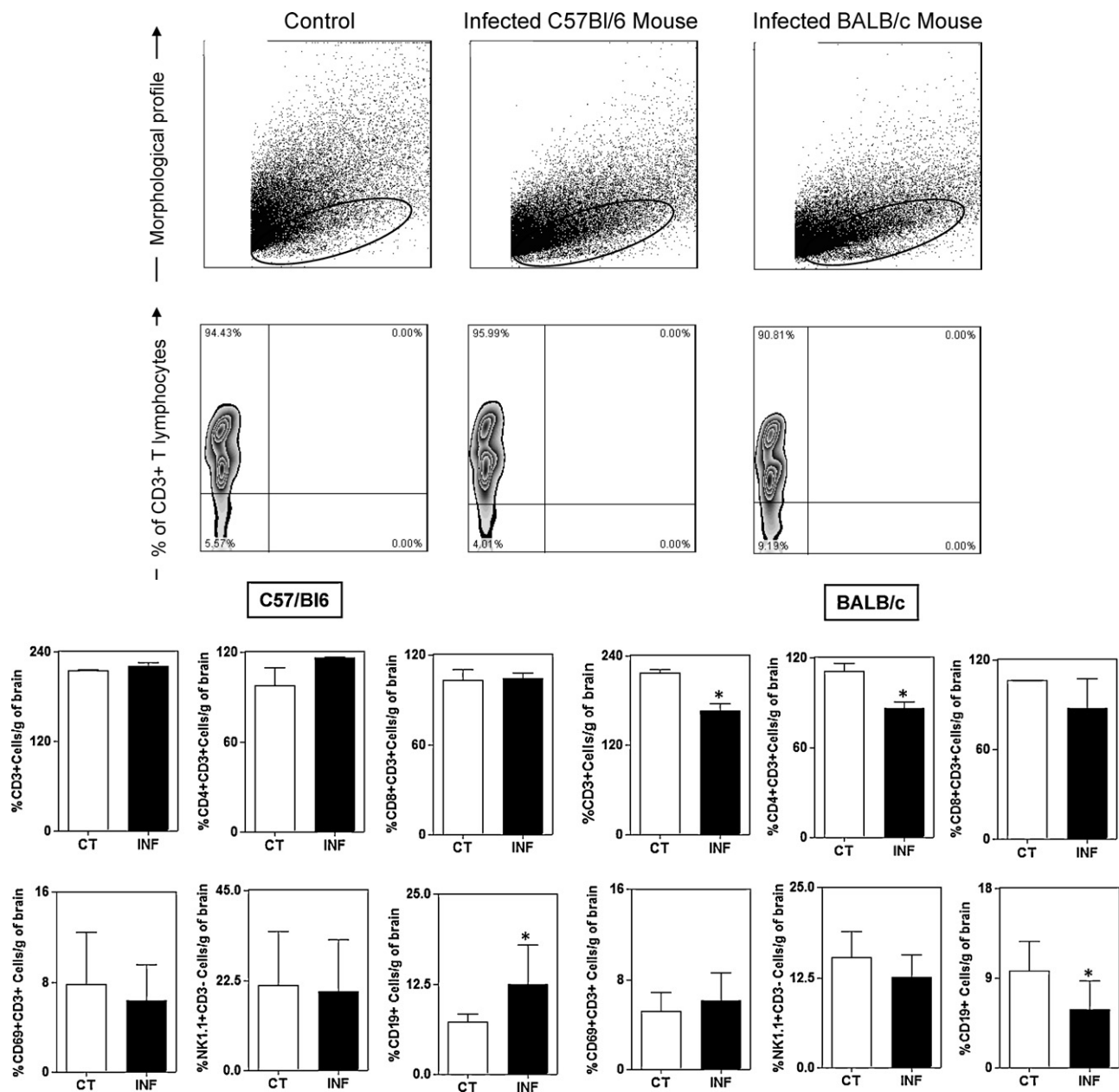
**Fig. 4.** The brain-sequestered lymphocytes (T CD3⁺ and their subsets CD4+ and CD8+ cells, T CD69⁺, NK CD3⁻NK1.1⁺ and B CD19⁺ cells) were detected in infected mice (INF) and control group (CT) as described in Section 2 and analyzed by flow cytometry. The cerebral percentage (% cells/g of brain) of B CD19⁺ lymphocytes is increased after *P. berghei* NK65 infection in C57Bl/6. In contrast, the cerebral percentage of T CD3⁺ lymphocytes as well as B CD19⁺ lymphocytes is decreased after *P. berghei* NK65 infection in BALB/c (B). Representative dot and zebra plots are shown (A). Each bar represents mean (n = 4/group) and ±SD values. Significant differences (p < 0.05) between infected and control mice are marked (*).

on 5 dpi, whilst the systemic, circulating levels of TNF-α were measured in serum samples. The concentration of the cytokine TNF-α in brain tissue of infected C57Bl/6 mice was significantly higher (p < 0.05) than in control samples (Fig. 6A). Whilst serum concentrations of TNF-α were significantly increased (p < 0.001) in both strains of infected animals in comparison with their respective controls (Fig. 6B), those in infected BALB/c mice were significantly higher (p < 0.01) than in infected C57Bl/6 animals.

Levels of the cytokine IFN-γ in the brain tissue of *P berghei* NK65 infected BALB/c mice were unchanged with respect to controls, although a significant increase (p < 0.05) was observed in infected C57Bl/6 animals in comparison with non-infected controls (Fig. 7A). The profiles of chemokines in brain samples derived from both strains of mice were somewhat different (Fig. 7B–F). In

BALB/c mice, levels of MIG/CXCL9 and MCP-1/CCL2 were increased after infection, but no significant changes were observed in the concentrations of KC/CXCL1, MIP-1α/CCL3 or RANTES/CCL5. In C57Bl/6 mice, infection led to significant increases in the levels of MIG/CXCL9, MCP-1/CCL2, MIP-1α/CCL3 and RANTES/CCL5 (Fig. 7).

## 4. Discussion

Murine models, involving experimental infection with malaria parasites isolated from thicket rats (*Thamnomys* spp.) in the African Congo, have been invaluable in studying the role of inflammatory and immune responses in the pathology of the disease (Beale et al., 1978). However, the intensity of disease pathology depends

on both the species of *Plasmodium* employed and on the strain of mouse infected (Grech et al., 2006). In the present study, C57Bl/6 and BALB/c mice were infected with the lethal strain *P. berghei* NK65 in order to assess any inflammatory changes in the cerebral microvasculature, without the typical signs of ECM.

After infection, progressive histopathological and immunological changes were observed in both strains, although parasitemia levels and survival did not show a direct relationship. On the other hand, the weight loss exhibited by animals of both strains following infection by *P. berghei* NK65 was correlated with high parasitemia. Although BALB/c mice infected with *P. berghei* NK65 exhibited equal or higher parasitemia and similar weight loss to infected susceptible C57Bl/6 mice, morphological changes in brain tissue were more intense and occurred earlier after infection in C57Bl/6 mice, and were accompanied by earlier mortality. These findings indicate a lack of correlation between parasitemia and the severity of pathological responses.

The induction of adhesion molecules on endothelial cells, as well as on the surface of leukocytes, during the inflammatory response favours the movement of leukocytes to the vessel walls and, consequently, facilitates leukocyte–endothelium interactions that lead eventually to extravascular migration (Piccio et al., 2002). In the present study, *P. berghei* NK65-infected BALB/c and C57Bl/6 mice exhibited levels of leukocyte rolling and adhesion in the cerebral microvasculature that were comparable with those reported earlier for mice experimentally infected with PbA (Chang et al., 2003). These results are also consistent with the histological analysis conducted in the present study, which indicated an inflammatory process in the brain following infection. However, the histological investigation and intravital microscopy revealed strain-related differences, with twice as many rolling leukocytes and around half the number of adherent cells in infected C57Bl/6 mice compared with infected BALB/c animals. The more extensive inflammatory response observed in the C57Bl/6 strain would be compatible with reports of its enhanced susceptibility to ECM (Hanum et al., 2003; Van den Steen et al., 2008).

Leukocyte infiltration into the brain parenchyma has been rarely observed but in the majority of studies leukocyte accumulation was found to occur intravascularly (Hearn et al., 2000). However, it is becoming increasingly accepted that cerebral malaria pathogenesis results from the sequestration of parasitized RBC as well as intravascular infiltration of host monocytes and lymphocytes within blood vessels in the brain. Recent studies indicated that T cells accumulate in brains of *P. berghei* - infected mice (Belnoue et al., 2002). Our results here showed an increased percentage of B CD19^{+} lymphocytes in *P. berghei* NK65-infected C57Bl/6 mice compared to control animals. However, T CD3^{+} lymphocytes were the most predominant cell types present on the brain leukocyte subpopulations in infected animals. Interestingly, a different phenomenon was observed in brain of mice infected with PbA. In that infection model, NK cells were found to migrate to the brains of malaria-infected animals, comprising a significant proportion of the total sequestered leukocyte pool. NK cells also stimulate recruitment of CXCR3-bearing T cells to the brain of animals with ECM (Hansen et al., 2007).

In addition, during inflammatory conditions of the CNS, a large number of mononuclear cells gain access to the CNS (Ransohoff, 2002). According to a number of authors (Piguet et al., 2000; Thumwood et al., 1988) the BBB is compromised following infection by PbA, possibly occasioned by endothelial damage caused by inflammatory mediators (Wassmer et al., 2006), and has been considered to be a major factor in the pathogenesis of CM (Hunt et al., 2006). In the present study, cerebral vascular permeability in experimental mice was observed to increase following infection by *P. berghei* NK65 and may be associated with the
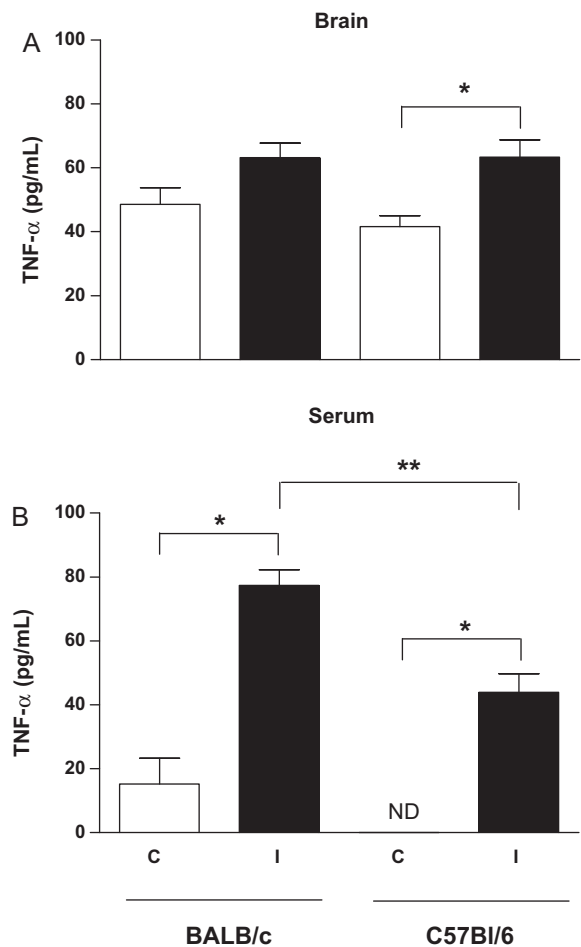


**Fig. 6.** Cerebral and systemic TNF-α concentrations (as determined by ELISA), showing protein concentration in brain tissue (panel A) and serum (panel B) of BALB/c and C57Bl/6 mice on day 5 after infection with *P. berghei* NK65 (bars labelled I) and in respective non-infected control mice (bars labelled C). Mean and ±SEM values for groups of at least six mice are shown (ND = not determined). The results were evaluated by ANOVA, with Bonferroni post-test. Significant differences ($p < 0.05$) between infected and control mice are marked (*), whilst differences between infected groups are marked (**).

oedema we observed and with the changes in lymphocytes in brain parenchyma.

Systemic and local inflammation appear to be orchestrated by the action of cytokines produced in response to infection. In the present study, increased levels of serum TNF-α were observed in infected mice of both strains. The significant increase in cerebral TNF-α observed in infected C57Bl/6 mice, but not in their BALB/c counterparts, corroborates published results from the more severe model of ECM (Lou et al., 1998). The TNF-α levels we found in infected C57Bl/6 mice may be related to the intense inflammatory histological changes observed at the same time, which were accompanied by earlier mortality. However, some studies have demonstrated no role for this cytokine in PbA-induced CM (Engwerda et al., 2002; Togbe et al., 2008).

IFN-γ can control the production of cytokines in the CNS and, additionally, is responsible for the specific migration to and intravascular sequestration of pathogenic CD8+ T cells in the brain of PbA-infected mice during ECM (Belnoue et al., 2008). In this context, cerebral IFN-γ levels were significantly increased in infected C57BL/6 mice at 5 dpi, whilst those in infected BALB/c animals remained similar to the corresponding control group.
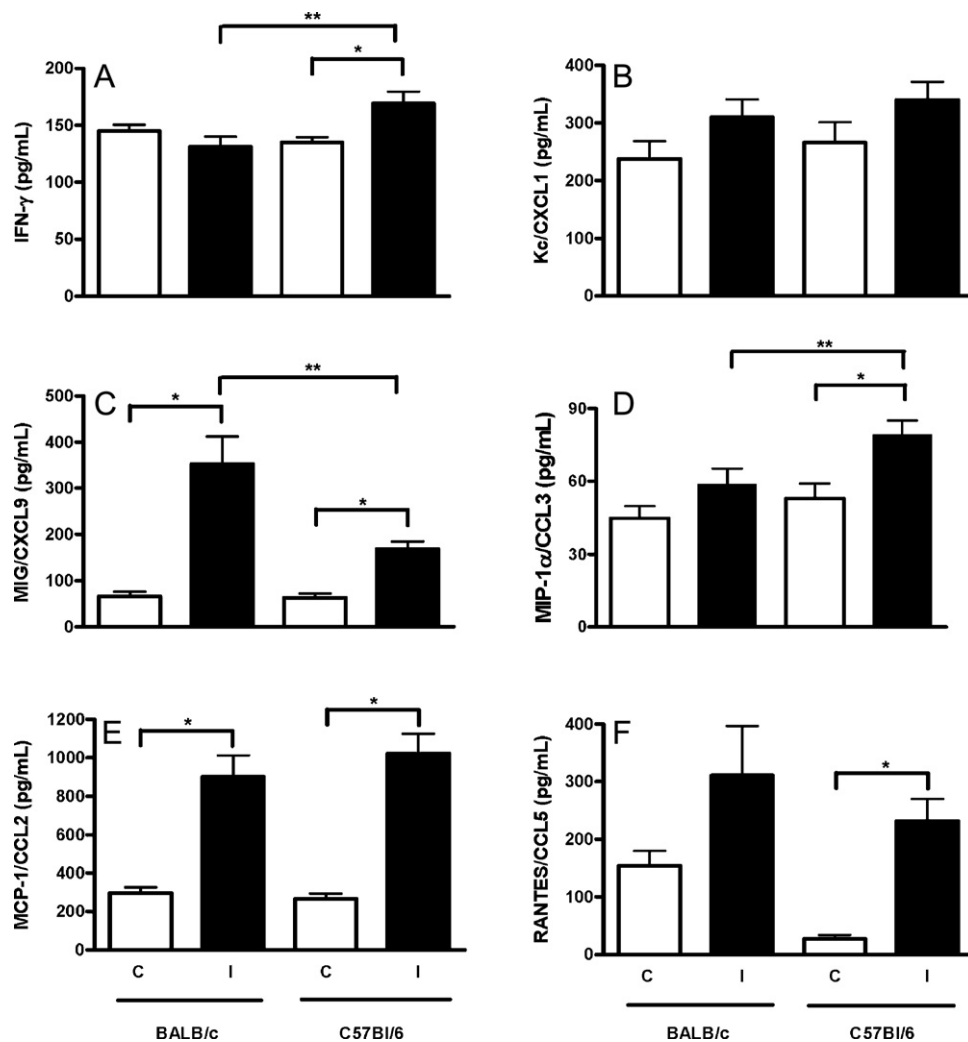
**Fig. 7.** Cerebral concentrations of IFN-γ, Kc/CXCL1, MIG/CXCL9, MIP-1α/CCL3, MCP-1/CCL2 and RANTES/CCL5 (as determined by ELISA), showing protein concentration in brain tissue of BALB/c and C57Bl/6 mice on day 5 after infection with *P. berghei* NK65 (bars labelled I) and in respective non-infected control mice (bars labelled C). Mean and ±SEM values for groups of at least seven mice are shown. The results were evaluated by ANOVA, with Bonferroni post-test. Significant differences ($p < 0.05$) between infected and control mice are marked (*), whilst differences between infected groups are marked (**).

Chemokines and chemokine receptors are regulators of leukocyte trafficking. Significant increases in RANTES/CCL5, MIP-1α/CCL3, MIG/CXCL9 and MCP-1/CCL2 were observed in infected C57BL/6 animals, but only the last two were significantly elevated in infected BALB/c mice. The chemokine profiles reported here are similar to those obtained in an earlier comparative study (Hanum et al., 2003) in which increases in the expression of mRNA of RANTES/CCL5, MCP-1/CCL2 and IP-10/CXCL10 were observed in both ECM-susceptible (C57BL/6) and resistant (BALB/c) mice that had been infected with PbA. In addition, a recent study revealed significant differences in mRNA expression levels of RANTES/CCL5, MCP-1/CCL2, IP-10/CXCL10, MIG/CXCL9, MIP-1β/CCL4 and I-TAC/CXCL11 in different *Plasmodium*/mouse strain combinations (Van den Steen et al., 2008). The differences in cerebral levels and profiles of chemokines between the two strains could explain their differences in susceptibility after infection, and also the histological changes observed in C57BL/6 mice as early as 5 dpi. Moreover, MCP-1/CCL2, a member of the CC chemokine family, can induce alterations in the vascular integrity of the BBB, thus promoting an increase in its permeability (Song and Pachter, 2004). This chemokine may therefore be involved in the increase of cerebral vascular permeability in C57BL/6 and BALB/c mice after infection by *P. berghei* NK65.

Whilst the malaria model involving infection with *P. berghei* NK65 produces no classical neurological indications of ECM, such as ataxia, paralysis, convulsions and coma followed by death (Bagot et al., 2002), the histological and intravital microscopy results obtained in the present study revealed clear signs of inflammation in the cerebral microvasculature in both strains of mice assayed. Thus there are inflammatory changes in the cerebral microvasculature, in the absence of the characteristic signs of ECM and when the lethality of the infection is related to organs outside the CNS (Van den Steen et al., 2010). Indeed, with *P. berghei* NK65 infection of C57BL/6 mice (Van den Steen et al., 2010), the cytokine and chemokine profiles in lung were comparable to those we found in brain, with increases in TNF-α, MCP-1 and KC. It may be that inflammatory changes in the cerebral microvasculature are not confined to CM models, but are to be found more widely among malaria strains, a possibility that requires further assessment. Nevertheless, we have shown that infection induced by *P. berghei* NK65 in mice culminated in an encephalitis that was associated with up-regulation of cerebral pro-inflammatory cytokines and chemokines, and intravascular inflammatory infiltrates in the cerebral tissue. Our results also suggest that *P. berghei* NK65 infection may result in an inflammation in the CNS that is not manifested as signs of neurological injury.

## Acknowledgments

## References

Baatz, H., Steinbauer, M., Harris, A.G., Krombach, F., 1995. Kinetics of white blood cell staining by intravascular administration of rhodamine 6G. Int. J. Microcirc. Clin. Exp. 15, 85–91.

Bagot, S., Campino, S., Penha-Gonçalves, C., Pied, S., Cazenave, P.A., Holmberg, D., 2002. Identification of two cerebral malaria resistance *loci* using an inbred wild-derived mouse strain. Proc. Natl. Acad. Sci. U. S. A. 99, 9919–9923.

Beale, G.H., Carter, R., Walliker, D., 1978. Genetics. In: Killick-Kendrick, R., Peters, W. (Eds.), Rodent Malaria. Academic Press, London, pp. 213–245.

Belayev, L., Busto, R., Zhao, W., Ginsberg, M.D., 1996. Quantitative evaluation of blood–brain barrier permeability following middle cerebral artery occlusion in rats. Brain Res. 739, 88–96.

Belnoue, E., Kayibanda, M., Vigario, A.M., Deschemin, J.C., van Rooijen, N., Viguier, M., Snounou, G., Rénia, L., 2002. On the pathogenic role of brain-sequestered alphabeta CD8+ T cells in experimental cerebral malaria. J. Immunol. 169, 6369–6375.

Belnoue, E., Potter, S.M., Rosa, D.S., Mauduit, M., Grüner, A.C., Kayibanda, M., Mitchell, A.J., Hunt, N.H., Rénia, L., 2008. Control of pathogenic CD8+ T cell migration to the brain by IFN-gamma during experimental cerebral malaria. Parasite Immunol. 30, 544–553.

Brenier-Pinchart, M.P., Pelloux, H., Derouich-Geurgour, D., Ambroise-Thomas, P., 2001. Chemokines in host protozoan parasite interactions. Trends Parasitol. 17, 292–296.

Carvalho-Tavares, J., Hickey, M.J., Hutchison, J., Michaud, J., Sutcliffe, I.T., Kubes, P., 2000. A role for platelets and endothelial selectins in tumor necrosis factor-alpha-induced leukocyte recruitment in the brain microvasculature. Circ. Res. 87, 1141–1148.

Chang, W.L., Li, J., Sun, G., Chen, H.L., Specian, R.D., Berney, S.M., Granger, D.N., van der Heyde, H.C., 2003. P-Selectin contributes to severe experimental cerebral malaria but is not required for leukocyte adhesion to brain microvasculature. Infect. Immun. 71, 1911–1918.

Clark, I.A., Ilschner, S., MacMicking, J.D., Cowden, W.B., 1990. TNF and *Plasmodium berghei* ANKA-induced cerebral malaria. Immunol. Lett. 25, 195–198.

de Souza, J.B., Riley, E.M., 2002. Cerebral malaria: the contribution of studies in animal models to our understanding of immunopathogenesis. Microbes Infect. 4, 291–300.

dos Santos, A.C., Roffê, E., Arantes, R.M., Juliano, L., Pesquero, J.L., Pesquero, J.B., Bader, M., Teixeira, M.M., Carvalho-Tavares, J., 2008. Kinin B2 receptor regulates chemokines CCL2 and CCL5 expression and modulates leukocyte recruitment and pathology in experimental autoimmune encephalomyelitis (EAE) in mice. J. Neuroinflamm. 5, 49.

Engwerda, C.R., Mynott, T.L., Sawhney, S., De Souza, J.B., Bickle, Q.D., Kaye, P.M., 2002. Locally up-regulated lymphotoxin alpha, not systemic tumor necrosis factor alpha, is the principle mediator of murine cerebral malaria. J. Exp. Med. 195, 1371–1377.

Grau, G.E., Piguet, P.F., Engers, H.D., Louis, J.A., Vassali, P., Lambert, P.H., 1986. L3T4+ T lymphocytes play a major role in the pathogenesis of murine cerebral malaria. J. Immunol. 137, 2348–2354.

Grau, G.E., Fajardo, L.F., Piguet, P.F., Allet, B., Lambert, P.H., Vassalli, P., 1987. Tumor necrosis factor (cachectin) as an essential mediator in murine cerebral malaria. Science 237, 1210–1212.

Grau, G.E., Piguet, P.F., Vassalli, P., Lambert, P.H., 1989. Tumor-necrosis factor and other cytokines in cerebral malaria: experimental and clinical data. Immunol. Rev. 112, 49–70.

Grau, G.E., Bieler, G., Pointaire, P., De Kossodo, S., Tacchini-Cotier, F., Vassalli, P., Piguet, P.F., Lambert, P.H., 1990. Significance of cytokine production and adhesion molecules in malarial immunopathology. Immunol. Lett. 25, 189–194.

Grech, K., Watt, K., Read, A.F., 2006. Host–parasite interactions for virulence and resistance in a malaria model system. J. Evol. Biol. 19, 1620–1630.

Hansen, D.S., Bernard, N.J., Nie, C.Q., Schofield, L., 2007. NK cells stimulate recruitment of CXCR3+ T cells to the brain during *Plasmodium berghei*-mediated cerebral malaria. J. Immunol. 178, 5779–5788.

Hanum, P.S., Hayano, M., Kojima, S., 2003. Cytokine and chemokine responses in a cerebral malaria-susceptible or -resistant strain of mice to *Plasmodium berghei* ANKA infection: early chemokine expression in the brain. Int. Immunol. 15, 633–640.

Hearn, J., Rayment, N., Landon, D.N., Katz, D.R., De Souza, J.B., 2000. Immunopathology of cerebral malaria: morphological evidence of parasite sequestration in murine brain microvasculature. Infect. Immun. 68, 5364–5376.

Hunt, N.H., Golenser, J., Chan-Ling, T., Parekh, S., Rae, C., Potter, S., Medana, I.M., Miu, J., Ball, H.J., 2006. Immunopathogenesis of cerebral malaria. Int. J. Parasitol. 36, 569–582.

Karunaweera, N.D., Grau, G.E., Gamage, P., Carter, R., Mendis, K.N., 1992. Dynamics of fever and serum levels of tumor necrosis factor are closely associated during clinical paroxysms in *Plasmodium vivax* malaria. Proc. Natl. Acad. Sci. U. S. A. 89, 3200–3203.

Laranjeiras, R.F., Brant, L.C., Lima, A.C., Coelho, P.M., Braga, E.M., 2008. Reduced protective effect of *Plasmodium berghei* immunization by concurrent *Schistosoma mansoni* infection. Mem. Inst. Oswaldo Cruz. 103, 674–677.

Lou, J., Gasche, Y., Zheng, L., Critico, B., Monso-Hinard, C., Juillard, P., Morel, P., Buurman, W.A., Grau, G.E., 1998. Differential reactivity of brain microvascular endothelial cells to TNF reflects the genetic susceptibility to cerebral malaria. Eur. J. Immunol. 28, 3989–4000.

Miller, L.H., Baruch, D.I., Marsh, K., Doumbo, O.K., 2002. The pathogenic basis of malaria. Nature 415, 673–679.

Ono, S.J., Nakamura, T., Miyazaki, D., Ohbayashi, M., Dawson, M., Toda, M., 2003. Chemokines: roles in leukocyte development, trafficking, and effector function. J. Allergy Clin. Immunol. 111, 1185–1199.

Pease, J.E., Williams, T.J., 2006. The attraction of chemokines as a target for specific anti-inflammatory therapy. Br. J. Pharmacol. 147 (Suppl. 1), S212–221.

Piccio, L., Rossi, B., Scarpini, E., Laudanna, C., Giagulli, C., Issekutz, A.C., Vestweber, D., Butcher, E.C., Constantin, G., 2002. Molecular mechanisms involved in lymphocyte recruitment in inflamed brain microvessels: critical roles for P-selectin glycoprotein ligand-1 and heterotrimeric Gi-linked receptors. J. Immunol. 168, 1940–1949.

Piguet, P.F., Da Laperrousaz, C., Vesin, C., Tacchini-Cottier, F., Senaldi, G., Grau, G.E., 2000. Delayed mortality and attenuated thrombocytopenia associated with severe malaria in urokinase- and urokinase receptor-deficient mice. Infect. Immun. 68, 3822–3829.

Ransohoff, R.M., 2002. The chemokine system in neuroinflammation: an update. J. Infect. Dis. 186 (Suppl. 2), S152–S156.

Saunders, N.R., Ek, C.J., Habgood, M.D., Dziegielewska, K.M., 2008. Barriers in the brain: a renaissance? Trends Neurosci. 31, 279–286.

Scheiermann, C., Colom, B., Meda, P., Patel, N.S., Voisin, M.B., Marrelli, A., Woodfin, A., Pitzalis, C., Thiemermann, C., Aurrand-Lions, M., Imhof, B.A., Nourshargh, S., 2009. Junctional adhesion molecule-C mediates leukocyte infiltration in response to ischemia reperfusion injury. Arterioscler. Thromb. Vasc. Biol. 29, 1509–1515.

Shaffer, N., Grau, G.E., Hedberg, K., Davachi, F., Lyamba, B., Hightower, A.W., Breman, J.G., Ngyen-Dinh, P., 1991. Tumor necrosis factor and severe malaria. J. Infect. Dis. 163, 96–101.

Snow, R.W., Guerra, C.A., Noor, A.M., Myint, H.Y., Hay, S.I., 2005. The global distribution of clinical episodes of *Plasmodium falciparum* malaria. Nature 434, 214–217.

Song, L., Pachter, J.S., 2004. Monocyte chemoattractant protein-1 alters expression of tight junction-associated proteins in brain microvascular endothelial cells. Microvasc. Res. 67, 78–89.

Teixeira-Carvalho, A., Martins-Filho, O.A., Andrade, Z.A., Cunha-Mello, J.R., Wilson, R.A., Corrêa-Oliveira, R., 2002. The study of T-cell activation in peripheral blood and spleen of hepatosplenic patients suggests an exchange of cells between these two compartments in advanced human *Schistosomiasis mansoni* infection. Scand. J. Immunol. 56, 315–322.

Togbe, D., de Sousa, P.L., Fauconnie, M., Boissay, V., Fick, L., Scheu, S., Pfeffer, K., Menard, R., Grau, G.E., Doan, B.T., Beloeil, J.C., Renia, L., Hansen, A.M., Ball, H.J., Hunt, N.H., Ryffel, B., Quesniaux, V.F., 2008. Both functional LTbeta receptor and TNF receptor 2 are required for the development of experimental cerebral malaria. PLoS ONE 3, e2608.

Thumwood, C.M., Hunt, N.H., Clark, I.A., Cowden, W.B., 1988. Breakdown of the blood–brain barrier in murine cerebral malaria. Parasitology 96, 579–589.

Van den Steen, P.E., Deroost, K., Aelst, I.V., Geurts, N., Martens, E., Struyf, S., Nie, C.Q., Hansen, D.S., Matthys, P., Van Damme, J., Opdenakker, G., 2008. CXCR3 determines strain susceptibility to murine cerebral malaria by mediating T lymphocyte migration toward IFN-gamma-induced chemokines. Eur. J. Immunol. 38, 1082–1095.

Van den Steen, P.E., Geurts, N., Deroost, K., Van Aelst, I., Verhenne, S., Heremans, H., Van Damme, J., Opdenakker, G., 2010. Immunopathology and dexamethasone therapy in a new model for malaria-associated acute respiratory distress syndrome. Am. J. Respir. Crit. Care Med. 181, 957–968.

Van Hensbroek, M.B., Palmer, A., Onyiorah, E., Schneider, G., Jaffar, S., Dolan, G., Memming, H., Frenkel, J., Enwere, G., Bennett, S., Kwiatkowski, D., Greenwood, B., 1996. The effect of a monoclonal antibody to tumor necrosis factor on survival from childhood cerebral malaria. J. Infect. Dis. 174, 1091–1097.

Wassmer, S.C., Combes, V., Candal, F.J., Juhan-Vague, I., Grau, G.E., 2006. Platelets potentiate brain endothelial alterations induced by *Plasmodium falciparum*. Infect. Immun. 74, 645–653.

World Health Organisation, 2000. Health Report 2000. Health Systems: Improving Performance. WHO, Geneva.

Yoshimoto, T., Takahama, Y., Wang, C.R., Yoneto, T., Waki, S., Nariuchi, H., 1998. A pathogenic role of IL-12 in blood-stage murine malaria lethal strain *Plasmodium berghei* NK65 infection. J. Immunol. 160, 5500–5505.